Temperature-Sensitive Poly(vinyl alcohol)/ Poly(methacrylate-*co*-*N*-isopropyl acrylamide) Microgels for Doxorubicin Delivery

Shivkumar V. Ghugare, Pamela Mozetic, and Gaio Paradossi*

Dipartimento di Scienze e Tecnologie Chimiche, and CRS SOFT CNR-INFM, Università di Roma Tor Vergata, 000133 Roma, Italy

Received February 11, 2009; Revised Manuscript Received April 8, 2009

Microgels based on poly(vinyl alcohol), PVA, grafted with methacrylate side chains, MA, incorporating *N*-isopropylacrylamide, NiPAAm, monomer, were prepared by water-in-water emulsion polymerization method. These systems exhibit a spherical shape and a volume-phase transition, that is, shrinking, below physiological temperature. The behavior of these microgels were studied with respect to their average size and size distribution, swelling, and release properties. It was observed that the stirring speed is a key parameter for controlling the amount of incorporated NiPAAm, the particle size and the sharpness of the volume-phase transition. The volume-phase transition temperature, VPPT, of the microgels was evaluated around 38 and 34 °C for microgels with a NiPAAm/methacrylate molar ratio of 0.8 and 2.4, respectively. Water uptake increased with the amount of NiPAAm monomer present in the polymer network. In vitro biocompatibility of microgels was assessed with respect to NIH3T3 mouse fibroblasts. *O*-Succinoylated microgels were loaded with doxorubicin by exploiting the favorable electrostatic interaction between negatively charged microgel surface and positively charged doxorubicin. The drug release was influenced by the microgels surface/volume ratio. At physiological temperatures, above the VPTT exhibited by these systems, the release was enhanced by the specific area increase. This study provides the background for the design of an injectable device suitable for the controlled delivery of doxorubicin based on the volume-phase transition of microgels.

Introduction

Fast response to external parameters is what makes a system "intelligent".[1,2] Design of the properties and functions of devices sensible to external gradients involves a number of different structural and dynamic parameters.[3] In the case of polymer hydrogels, the main contribution to the response is a volume transition that can be triggered by pH, ionic strength, and temperature.[4–7] Responsivity to these stimuli are largely amplified by the connectivity characterizing a chemically cross-linked hydrogel. The presence of fixed and ionizable charges in the polymer network makes possible the triggering by pH and ionic strength, whereas the temperature transition is caused by the presence of residues displaying a thermally sensible behavior in the polymer network due to the interpolymer chain association through hydrophobic interaction. Focusing on networks featuring this latter effect, the choice of possible monomers to use as building blocks of the responsive polymer network is greatly limited by environment and temperature conditions in which the device is designed to function. When responsivity is combined with a high value of specific surface, exchange processes will be largely enhanced.[4,8–11] This can be achieved by colloidal microdevices such as microgels, where a favorable large surface/volume ratio can enhance the bioavailability of the drug playload.[12]

The microgel particles are designed as injectable drug deliverable systems for parenteral administration. For this kind of application, requirements are the nano/micro overall size and a large water volume fraction to preserve the conformational state of the drug payload.[8–11,13]

The interaction with cells is one of the processes occurring as soon as the microgels are injected in the bloodstream.[14] Devices based on soft matter are attractive because of their unique chemical and physical versatility for conjugating molecules able to promote adhesion to targeted cells and to allow local drug delivery. However, this suitability is counterbalanced by the general requirements involving biocompatibility of the material used for designing the sphere microgels.

The use of NiPAAm as a key monomer for assigning thermal responsivity to the network has been often made. The lower critical solution temperature, LCST, occurring in poly(NiPAAm) aqueous solution around 32 °C,[15] is at the base of a volume-phase transition displayed in hydrogels containing cross-linked poly(NiPAAm) and has been used to design the organic component in hybrid devices incorporating quantum dots.[16] Recently, the structure of poly(NiPAAm) microgels in aqueous suspensions has been determined.[17,18] The dynamics of the polymer chains around the transition temperature[19] and of the solvent confined in the network[20] have been investigated by incoherent quasi elastic neutron scattering and by NMR ^{1}H spin−spin relaxation time measurements, respectively.

The temperature transition is influenced by factors as pH, ionic strength, and presence of comonomers. However, in many cases, VPTT is close or coincident with physiological temperature conditions.[21] This background suggests that loaded nano/micro systems could undergo significant size changes with an efficient release of the drug payload making microgels attractive for the design of injectable devices with tailored features.

Our previous experience in fabrication of microgels[22] with good colloidal stability based on a methacryloyl-derivatized poly(vinyl alcohol) network[23] by water-in-water microemulsions provided the background for incorporating NiPAAm in the

* To whom correspondence should be addressed. E-mail: paradossi@stc.uniroma2.it.

10.1021/bm900185u CCC: $40.75
Published on Web 05/08/2009

network to obtain thermal responsivity to the resulting microgels. It should be stressed that this water-in-water microemulsion polymerization has the remarkable advantage to use nontoxic chemicals throughout the synthesis. This assures that the resulting microgels will not release harmful molecules during their functioning. Moreover, the use of a poly(vinyl alcohol), PVA, based drug delivery microgels should allow for a low, if any, cytotoxic impact on cells.

We addressed this work to the design of smart, that is, stimuli-responsive, drug delivery microgels, testing their biocompatibility and ability to control the drug release with an anticancer case molecule as doxorubicin.

Thermal response of the microgels can also be considered for the design of nano/micro temperature sensors as it will be illustrated in a next paper. Here we focus on the structural and thermal features of PVA/Poly($MA_mNiPAAm_n$) microgels.

Experimental Section

Materials. *N*-Isopropyl acrylamide (NiPAAm), purchased from Aldrich chemicals, was recrystallized in *n*-hexane prior to use. All other chemicals were used as received. Poly(vinyl alcohol) with number and weight average molecular weights of 30000 ± 5000 and 70000 ± 10000 g/mol, respectively, dextranT40 and blue dextran, with a number average molecular weight of 35000−40000 and 2000000 g/mol respectively, succinic anhydride and phosphate-buffered saline (PBS) were purchased from Sigma.

4-(*N*,*N*-Dimethylamino) pyridine (DMAP), glycidylmethacrylate (GMA), and fluorescein isothiocynate isomer 1 (FITC) were Fluka products. Photoinitiator 2-hydroxy-1-[4-(hydroxyethoxy)phenol]-2-methyl 1-propanone (Irgacure 2959) was purchased from Ciba.

Dimethyl sulfoxide (DMSO), inorganic acids, and bases were RPE grade products supplied by Carlo Erba.

Dulbecco's modified Eagle's medium (DMEM), L-glutamine 200 mM, and penicillin/streptomycin solution, at a concentration of 10000 U/mL and 10 mg/mL, respectively, were purchased from HyClone. Fetal bovine serum and MTT (3-(4,5-dimethylthyazol-2-yl)-2,5-diphenyltetrazolium bromide) were Sigma products.

Water was Milli-Q purity grade (18.2 MΩ·cm) produced with a deionization apparatus (PureLab) from USF, Elga. Dialysis membranes (cut off 12000 g/mol) were purchased from Medicell International Ltd. and prepared according to standard procedure.

Methods. *Synthesis of Poly(vinyl alcohol)-methacrylate (PVA-MA).* PVA was grafted with glycidylmethacrylate according to the procedure described elsewhere.[24–26] Briefly, 10 g of PVA was dissolved in 250 mL of DMSO at 70 °C. After complete dissolution of PVA, the flask was cooled to room temperature, and then 5 g DMAP was added under N_2 flux. After 1 h, a known amount of GMA was added in the proper molar ratio with respect to polymer repeating unit. The reaction was carried out at room temperature in darkness with stirring and stopped after 48 h by neutralizing the solution with an equal molar amount of HCl with respect to DMAP. DMSO was replaced with water by exhaustive dialysis. The sample was stored as a freeze-dried powder. After methacryloyl grafting, the degree of substitution (DS) was determined by ^{1}H NMR analysis.[24] For microgel preparation, a sample with DS 4.7%, hereafter labeled PM5, was used throughout this study.

Preparation of Microgels. Microgels based on PM5 were prepared, adapting a procedure originally introduced by Franssen and Hennink,[22,27] which employs a water-in-water emulsion technique based on polymer−polymer immiscibility in aqueous solutions. In a typical experiment, an aqueous dispersion containing dextran T40 at a concentration of 16% (w/v), PM5 at 2% (w/v), and the UV photoinitiator Irgacure 2959 at 0.3% (w/v) was vigorously stirred by an UltraTurrax at 8000 rpm. After emulsification, PM5 in the dispersed phase was cross-linked by photopolymerization using a 365 nm light source at an intensity of 7 mW/cm^2 for 5 min. NiPAAm monomers, present in both aqueous phases, were cross-linked in the PM5 containing phase because of the availability of vinyl moiety grafted to PVA chains. The cross-linked PVA/Poly(methacrylate-*co*-*N*-isopropyl acrylamide) microgels were purified by repeated steps of centrifugation and resuspension in Milli-Q water. Microgels prepared at 8000 and 16000 rpm will be hereafter labeled PMN-I and PMN-II, respectively. Microgels prepared at 8000 rpm following this procedure in the absence of NiPAAm[22] will be labeled PM-I.

Preparation of Negatively Charged Microgels. Details on the preparation of negatively charged PM-I type microgels has been already reported[22] and was also applied to PMN-I and PMN-II. Typically, 1 g of PMN microgels and 0.5 g DMAP were suspended in 25 mL of anhydrous DMSO and stirred under N_2 flux. After 1 h, succinic anhydride (0.25 g) was added, keeping the suspension at 40 °C for 48 h under a nitrogen atmosphere. The reaction was stopped by neutralization and the suspension was dialyzed against Milli-Q water. The degree of *O*-succinoylation of the microgels, determined by potentiometric titration, was 10 ± 2 mol % with respect to PVA repeating units.

Determination of the Morphology and Size Distribution of Microgels. Freeze-dried PMN-I and PMN-II microgels were first immersed in Milli-Q water at room temperature to reach their equilibrium state. Then, the swollen microgels were labeled with FITC by coupling the dye to PVA hydroxyl group.[28] Fluorescent dye at a concentration of 10 μM was added in the dispersion. The excess dye was removed by repeated washings with Milli-Q water, and CLSM observations were performed using a confocal laser scanning microscope (Nikon PCM 2000, Nikon Instruments, Japan) with a 60×/1.4 oil immersion objective. The 488 nm line of 100 mW argon ion laser was used for sample fluorescence excitation of PMN-I and PMN-II microgels. Images were collected with a pixel size of 0.414 μm using the entire field of 512 × 512 pixels. Microgels average diameter and standard deviation were determined over a set of 100 and 200 microgel images of PMN-I and PMN-II, respectively, using ImageJ software package (http://rsb.info.nih.gov/ij/).

Thermoresponsiveness of Microgels. Thermoresponsiveness of PMN-I and PMN-II microgels was evaluated by dynamic light scattering (DLS) method, using a BI-200SM goniometer (Brookhaven Instruments Co.) equipped with a laser source at 532 nm, coupled with a temperature controller. The temperature was controlled from 20 to 43 °C. The autocorrelation functions were analyzed with the CONTIN algorithm.

Fourier Transform Infrared Analysis. Freeze-dried samples of PMN-I and PMN-II microgels were analyzed in nujol by using an FT-IR spectrophotometer NEXUS THERMO Nicolet.

Elemental Analysis. Elemental analysis was carried out on freeze-dried microgels by using a Thermo Finnigan Flash Elemental Analyzer-1112 instrument.

Differential Scanning Calorimetry (DSC). Volume phase transitions temperature of the PMN-I and PMN-II were examined using a TA Q2000 differential scanning calorimeter. Known amounts of dry microgels were equilibrated in Milli-Q water at room temperature to reach the maximum swelling and centrifuged to eliminate the excess of water. An exactly weighted amount of slurry, about 10−15 mg, was placed inside an aluminum pan and then hermetically sealed with an aluminum lid. The scans were performed from 25 to 55 °C on the swollen microgels at a heating rate of 3 °C/min under a flux of 50 mL/min of dry nitrogen.

Swelling Kinetics of Microgels. The swelling kinetics of PM-I, PMN-I, and PMN-II microgels were studied applying the method outlined by Hennink et al.[29] In a typical swelling experiment, 10 mg of dry microgels were immersed in 2 mL of 7×10^{-5} M blue dextran solution. The concentration of blue dextran at time t (min), C_t, was monitored by measuring the absorbance at $\lambda = 620$ nm by JASCO 7850 double beam UV−vis spectrophotometer. The water uptake by dry microgels (W) was determined as

$$\text{water uptake}(W) = [V_i - (BD/C_t)]/a$$

where V_i is the initial volume of blue dextran solution (mL), BD is the initial molar amount in the blue dextran solution in the presence of microgels, and a is the amount of dry microgels (g).

Doxorubicin Loading. In a typical doxorubicin (DOXO) loading experiment, 10 mg of freeze-dried *O*-succinoylated microgels was suspended in 3 mL of aqueous DOXO at a concentration of 1.70×10^{-4} M and left for 12 h under gentle stirring. Then microgels were centrifuged and the absorbance of supernatant was measured at 485 nm with a JASCO 7850 double beam UV−vis. Determination of the DOXO payload was based on a molar extinction coefficient value of $\varepsilon_{485} = 11500\ M^{-1} \cdot cm^{-1}$. Finally, DOXO-loaded microgels were freeze-dried for release studies.

Doxorubicin Release Kinetics. Typically, 10 mg of freeze-dried DOXO loaded microgels immersed in 3 mL of PBS solution at a controlled temperature of 20 and 37 °C. At regular times the supernatant from each sample was removed after centrifugation and replaced with the same amount of fresh PBS solution. DOXO release was monitored by measuring the time dependence of the absorbance at 485 nm. Release behavior was analyzed in terms of cumulative ratio (%) of released DOXO.

NIH3T3 Mouse Fibroblasts Culturing. NIH3T3 mouse fibroblasts were purchased from Istituto Zooprofilattico Sperimentale della Lombardia e dell'Emilia Romagna "Bruno Umbertini", Brescia, Italy. The cells were maintained in complete medium consisting of DMEM supplemented with 2 mM L-glutamine, 10% heat-inactivated fetal bovine serum, and 1% antibiotic mixture, consisting of 100 U/mL of penicillin and 100 μg/mL of streptamycin. Cells were cultured in a humidified 5% CO_2 atmosphere at 37 °C. The fibroblasts were plated at known concentration in 24-well plates and let adhere for 24 h before use.

MTT (Methylthiazole Tetrazolium) Cytotoxicity Assay. The MTT assay[30] provides a quantitative determination of viable cells. NIH3T3 mouse fibroblasts were seeded at a density of 50000 cells per well into 24 well plates and allowed to adhere for 24 h at 37 °C in the presence of 5% CO_2. After 1 day, cells were incubated with microgels for 4, 8, and 18 h in serum-free media. Cytotoxicity was assessed by MTT assay. MTT solution was added to a final concentration of 0.5 mg/mL to each well and incubated for 4 h at 37 °C. The formazan crystals formed as byproduct of MTT reaction with cells were dissolved in 200 μL of DMSO, and absorbance was recorded at 570 nm.

In Vitro Proliferation Studies. NIH3T3 mouse fibroblasts in exponential growth phase were washed, trypsinized, and resuspended in serum-free medium. Each well contained approximately 50000 cells and incubated for 24 h during which a monolayer was partially formed. The cells were than exposed to various quantities and types, typically 25 and 50 μg of microgel suspension in 0.5 mL of complete medium, and the plates were incubated at 37 °C, 5% CO_2, for 1, 3, and 7 days. At the end of each day, MTT solution was added to a final concentration of 0.5 mg/mL in each well and incubated for 4 h at 37 °C. The formazan crystals formed as byproduct of MTT reaction with cells were dissolved in 200 μL of DMSO and absorbance was recorded at 570 nm.

For both cytotoxicity and proliferation studies, microgels were sterilized in 70% EtOH for two days and then equilibrated in sterile PBS. In these experiments the absorbance values of DMSO/formazan solutions were converted into the corresponding number of cells by means of a linear calibration by carrying out the MTT test on a known number of cells (typically 50000).

Results and Discussion

Water-in-water microemulsion has been proven to be a handy and safe approach to provide microgels based on polymer incompatibility.[27,31] We have used this method for the obtainment of microgels able to control the release of doxorubicin to tumor cells. The addition of NiPAAm as comonomer in the emulsion at room temperature was attempted to copolymerize this molecule with the methacryloyl side chains of the grafted PVA, PM5, to impart temperature sensitivity at physiological conditions to the PVA-based microgels (Scheme 1).

As starting material, we used PVA with a methacryloyl substitution of 5%, PM5, determined by ^{1}H NMR spectroscopy.

Scheme 1. Chemical Structure of PVA/Poly(MA_mNiPAAm_n) Network

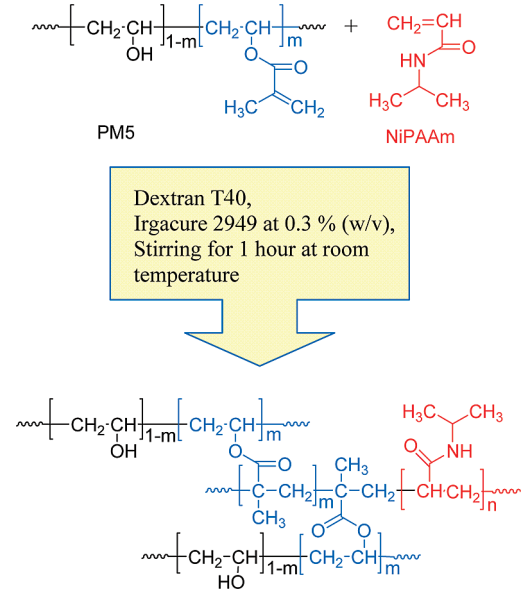

Due to the low solubility of the polymer in water, higher degrees of substitution could not be used.

NiPAAm was added in the water-in-water emulsion under high shear stirring, and incorporation in the PM5 containing phase was carried out by photopolymerization with UV irradiation in the presence of Irgacure 2959.

The incorporation of NiPAAm in PMN-I and PMN-II microgels was detected by FT-IR spectroscopy (Figure 1). Peaks at 1645 and 1545 cm^{-1} due to amide I and amide II, respectively, are present in the NiPAAm containing samples, whereas a peak at 1706 cm^{-1} showed the presence of the ester group common to all the samples, that is, PMN-I, PMN-II, and PM-I, due to the methacryloyl-substituted PVA.

Elemental analysis confirmed the incorporation of NiPAAm in the polymer network and showed that the amount of cross-linked NiPAAm was dependent on the shear stirring rate, as summarized in Table 1. At a stirring speed of 8000 rpm, and 16000 rpm the amount of NiPAAm incorporated in the microgels was 0.8 and 2.4 per moles of methacrylate moiety, respectively, regardless of the initial NiPAAm monomer content in the emulsion, indicating a saturation effect of NiPAAm solubility within the PM5 rich phase. An increase in the stirring speed is relevant in determining the amount of incorporated NiPAAm as a higher sheer stirring corresponded to an increase of the NiPAAm content in the network (see Table 1). The more efficient monomer embodiment in the vinyl rich phase when

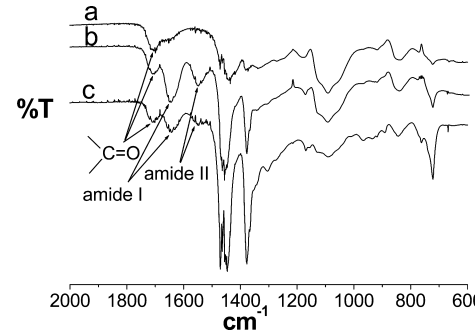

Figure 1. FT-IR spectra of (a) PM-I, (b) PMN-I, and (c) PMN-II microgels.

Table 1. Elemental Analysis on Different PVA/poly(MA-*co*-NiPAAm) Samples

microgel type	stirring speed (rpm)	C (%)	H (%)	N (%)	NiPAAm/MA (molar ratio)	NiPAAm in matrix (wt %)
PM-I	8000	54.73	10.02	absent	0	0
PMN-I	8000	51.70	9.49	1.04	0.8	9
PMN-II	16000	53.54	9.69	2.72	2.4	22

the stirring speed is higher is probably due to the larger specific surface available in this condition.

In Figures 2a,b and 3a,b particle size and size distribution of microgels were studied by confocal laser scanning microscopy, CLSM. PMN-I and PMN-II microgels showed diameter values around 4 and 1.6 μm, respectively, with a relatively narrow size distribution. The size of the microgel particles strongly depended on stirring speed: by increasing the stirring speed from 8000 to 16000 rpm, the size of the microgels decreased by 50% due to the breaking down of the larger droplets of the dispersion.

The dynamic light scattering (DLS) autocorrelation functions of the scattered intensity of microgel aqueous dispersions were studied in order to assess the hydrodynamic diameters of PMN-I and PMN-II particles as well as their size distribution. In Table 2 the dependence of the average particle size from the shear rate applied to the emulsion during the photoinitiated cross-linking reaction is summarized.

The analysis of the DLS correlation functions of PMN-I microgel by means the cumulants method, revealed the presence of a not negligible population of particles with diameter of 8 ÷ 10 μm. We exclude that this contribution was due to the presence of hydrogel debris in the dispersion. As shown in Figure. 2a, irregularly shaped polymeric particles are not present in PMN-I aqueous dispersion. Moreover, the tailed shape of the size distribution of PMN-I were also confirmed by the CLSM analysis, see Figure. 2, b.

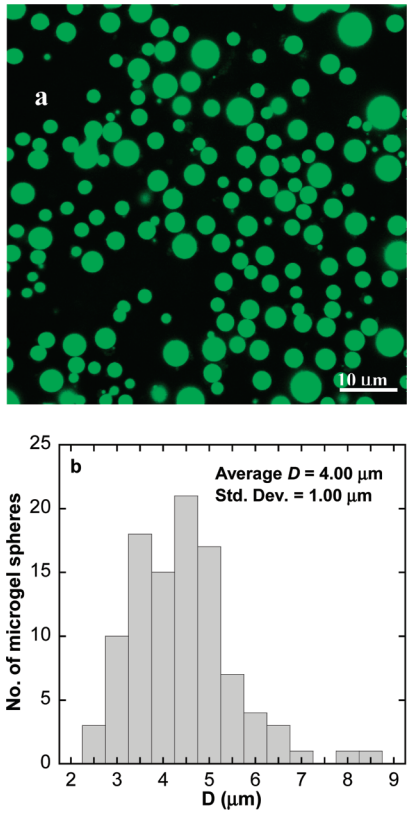

Figure 2. CLSM image (a) and size distribution (b) of PMN-I.

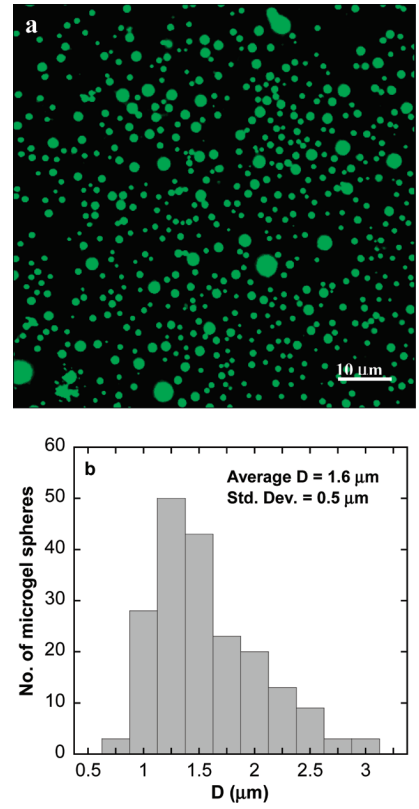

Figure 3. CLSM image (a) and size distribution (b) of PMN-II.

Table 2. Confocal Laser Scanning Microscopy (CLSM) and DLS Average Diameters of PMN-I and PMN-II at Room Temperature

microgel type	stirring speed (rpm)	CLSM D_z[a] at RT (μm)	DLS D_h at RT (μm)
PMN-I	8000	4.0 ± 1.0	4.0 ± 0.6
PMN-II	16000	1.6 ± 0.5	1.65 ± 0.2

[a] z-Average is reported for comparison with the D_h determined by DLS.[32]

On the other hand, the microgels PMN-II, prepared at higher shear stirring, that is, 16000 rpm, showed a smaller average size with limited tailing of the distribution.

From this analysis we assessed the relevant effect of the stirring speed on the size of the microgels and, therefore, the possibility to tailor the particle dimensions by applying the proper shear rate to the emulsion. Moreover, the results concerning the average diameter and the narrow size distribution open the possibility of using microgels as injectable drug delivery system.

The temperature sensitivity of PMN-I and PMN-II microgels was studied by performing a DLS investigation of the particles dimensions as a function of temperature. The study of changes in the size distribution of PMN-I with temperature, reported in Supporting Information, clearly showed that the small fraction of microgels constituting the tail of PMN-I distribution is not temperature responsive. However, microgels included in the $D_h \pm \sigma$ size range and representing about 80% of the overall PMN-I sample population were thermally sensible (see Supporting Information).

Selecting only this population, the temperature dependence of the average hydrodynamic diameter was determined as shown in Figure 4, evaluating the midpoint of the DLS average diameters versus temperature curves as the volume-phase transition temperature, VPTT. According to this analysis, the transition temperature occurred at about 33 °C upon heating

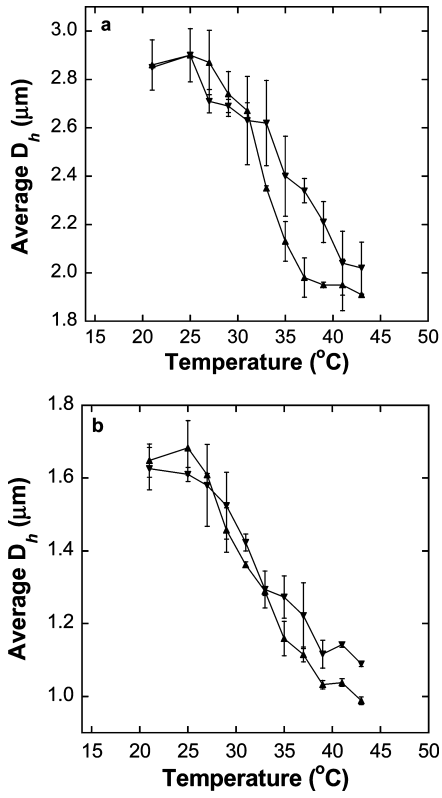

Figure 4. Hydrodynamic diameter of (a) PMN-I and (b) PMN-II microgels as a function of temperature. ▲heating; ▼cooling.

Table 3. Hydrodynamic Diameters, D_h, by DLS at Room Temperature (RT) and at 43 °C

microgel type	stirring speed (rpm)	DLS D_h at RT (μm)	DLS D_h at 43 °C (μm)	shrinking ratio[a]
PMN-I	8000	4.0 ± 0.6	2.0 ± 0.6	0.125
PMN-II	16000	1.65 ± 0.2	0.8 ± 0.1	0.114

[a] Defined as $D_{collapsed}/D_{swelled}$.[3]

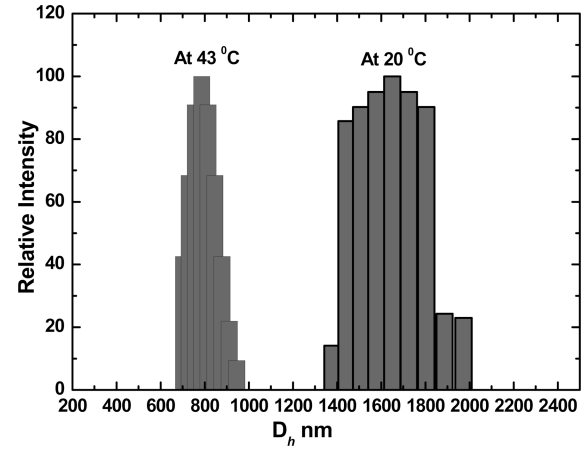

Figure 5. Hydrodynamic diameter of PVA/P(MMA-*co*-NiPAAm) microgel PMN-II at room temperature and 43 °C.

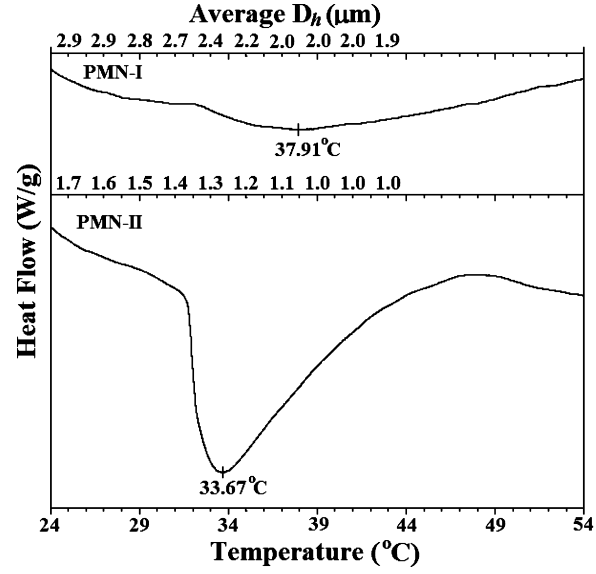

Figure 6. DSC thermograms of PMN-I and PMN-II microgels.

and at 37 °C upon cooling, with a hysteresis of about 4 °C. The temperature dependence of the size distribution of PMN-I microgel particles population sensible to temperature is reported in Supporting Information at room temperature and 43 °C.

The thermal behavior of PMN-II was homogeneous over the whole microgel sample. The volume-phase transition of PMN-II occurred at temperature of 33 °C without detection of hysteresis behavior. As summarized in Table 3, PMN-I and PMN-II displayed a decrease in size by increasing the temperature with a larger value of the shrinking ratio for the network, PMN-II, containing a higher amount of NiPAAm.

PMN-II size distribution at room temperature and at 43 °C, obtained by CONTIN analysis of the DLS correlation functions, is shown in Figure 5.

The volume-phase transition was accompanied by a heat effect clearly detected by differential scanning calorimetry (DSC). PMN-I and PMN-II slurries exhibited endothermic peaks with maxima corresponding to temperatures of 38 and of 34 °C, respectively (Figure 6). According to DLS, at these temperatures the volume-phase transition was nearly completed. The DSC behavior of poly(vinyl alcohol)/poly(methacrylate-*co*-*N*-isopropyl acrylamide) network depends from factors as the chemical composition and the distribution of the NiPAAm monomer with respect to PVA chains and by the balance between the hydrophobic/hydrophilic residues in the polymer network. In monolithic hydrogels reported by Feil et al.,[33] the presence of hydrophilic moieties in polymer networks containing NiPAAm caused an increase of the LCST value in comparison with the value found with poly (NiPAAm).

For our microgels, the enthalpy change related to the volume phase transition was 14.6 and 13.2 J/g of NiPAAm for PMN-I and PMN-II, respectively, in agreement with DSC results of poly(NiPAAm-*co*-methacrylic acid) macroscopic hydrogels.[34]

The swelling kinetics of PMN-I and PMN-II microgels at room temperature were compared with the time dependence of PM-I microgels swelling. In Figure 7, the degree of swelling, W, is reported as a function of time.

The data can be described by a swelling process with a second-order kinetics[35]

$$\frac{dW}{dt} = K(W_\infty - W)^2 \quad (1)$$

Integration with respect to time of eq 1 yields

$$W = \frac{KW_\infty^2 t}{1 + KW_\infty t} \quad (2)$$

It is important to stress the heuristic meaning of eqs 1 and 2 as they refer to the swelling, a complex process made of several microscopic steps involving hydrogen bonding, rearrangements

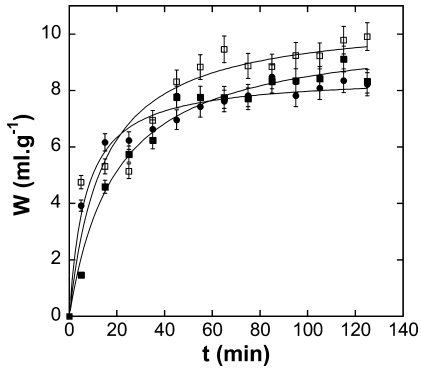

Figure 7. Swelling kinetics of (●) PM-I, (■) PMN-I, and (□) PMN-II microgels.

Table 4. Kinetic Parameters of the Swelling Process of Microgels

microgel type	equilibrium water content W_∞	specific rate constant K $(\text{concn}\cdot\text{min})^{-1}$
PM-I	8.5	0.0170
PMN-I	10.2	0.0055
PMN-II	10.6	0.0070

and disentanglements of chains, and solvent penetration. Equation 2 offers a satisfactory fit of the swelling data, with a higher value of W_∞ for PMN-I and PMN-II compared to PM-I, and it allows the evaluation of the amount of water uptake at equilibrium, W_∞, and of the observed rate constant of the process, K. Table 4 summarizes the relevant parameters of the swelling kinetics of PM-I, PMN-I, and PMN-II.

The difference in water uptake between PMN-I and PMN-II microgels was not significant. On the other hand, PMN-I and PMN-II, W_∞, was higher than for PM-I. This can be explained considering that poly(NiPAAm) is a water-soluble polymer exhibiting a disordered extended chain conformation below LCST and allowing the microgel to bind more water molecules, resulting in a greater water uptake.[36] However, as indicated by the specific rate constants of PMN-I and PMN-II, water penetration in these networks was slower compared to the PVA/poly(methacrylate) network due to the higher amount of heterogeneities of the NiPAAM containing networks.

To investigate the influence of the temperature on the release properties of PMN-I and PMN-II microgels, the networks were loaded with doxorubicin, one of the most common anticancer drugs. To optimize the cargo payload, we adopted the same strategy used for PM-I microgels,[22] conjugating succinoyl groups to the hydroxyl moiety of the microgel. In this way, PMN-I and PMN-II microgels were functionalized with a 10% of O-succinoylation with respect to PVA repeating units. This substitution provided a negative charge density, favoring the adsorption of doxorubicin molecules bearing positively charged amine groups at physiological pH. The loading was accomplished by suspending the microgels in an aqueous solution of doxorubicin. Loaded microgels were stored as freeze-dried powder. In PBS medium succinoylated PMN-I and PMN-II microgels released DOXO as described in Figure 8. A loading capacity of about 90% of the microgels dry weight was determined. This results was used for the evaluation of the cumulative release of DOXO (see below).

For both types of microgels, the amount of released drug after 60 min at room temperature was 40 and 45% for succinoylated PMN-I and PMN-II, respectively, indicating a more efficient drug release at equilibrium for the system having the higher specific surface. This difference increased markedly at 37 °C

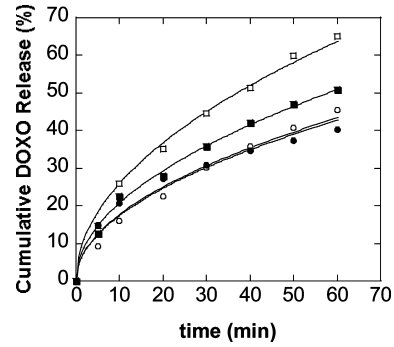

Figure 8. Doxorubicin release kinetics of PMN-I (full symbols) and PMN-II (empty symbols) at room temperature (circles) and at 37 °C (squares).

where the cumulative release at equilibrium is 65% against 50% in favor of succinoylated PMN-II. At this temperature, both types of microgels completed the volume-phase transition and the larger release of doxorubicin exhibited by PMN-II corresponded to a more pronounced shrinking effect occurring in this system (see Table 3). The DOXO release by succinoylated PMN-I and PMN-II was directly related to the swelling state of microgels, rather than to skin formation effect.[37] Only in gels phases containing more than 90% NiPAAm, skin formation can function as a rate controlling factor of the exchange processes occurring at the gel surface.[37,38] The more efficient drug release exhibited by PMN-I and PMN-II at higher temperature was the result of the increased hydrophobicity of the microgel networks at 37 °C, making less favorable the interaction with charged DOXO molecules and of the increase of the specific area due to the volume-phase transition occurring in both microgels when suspensions are brought from room to physiological temperature. At 37 °C, the comparison of the releases by the two types of microgels suggests that the difference in the shrinking factor (see Table 3) again plays a key role as far as the release efficiency is concerned.

Considering that microgels have been designed for parenteral administration, the biocompatibility of this device was investigated by studying the viability and proliferation of NIH3T3 mouse fibroblasts in the presence of PM-I, PMN-I, and PMN-II microgels.

Cytotoxicity of microgels was assessed as a function of time and of particles concentration. NIH3T3 cells were seeded in DMEM and were cultured in the presence of different microcapsules amount (0, 5, 10, 20, 40, and 50 μg/well, each well containing 0.5 mL of suspension) for each type of microgels. Both assays were performed by MTT test consisting in the conversion of this reactant into water-insoluble formazan crystals by mitochondrial dehydrogenases of living cells.

NIH3T3 mouse fibroblasts incubated for 4, 8, and 18 h with different amounts of PM-I, PMN-I, and PMN-II microgels were tested by MTT assay to measure cell viability. As shown in Figure 9, PM-I and PMN-I microgels did not influence the fibroblasts viability up to a concentration of 40 μg/well. A limited decrease in the viability was detected when cells were treated with PMN-I microgel at a concentration of 50 μg/well or with PMN-II microgel at all concentrations. Viability evaluations were performed with respect to the results obtained on cells incubated in the absence of microgels.

The proliferation activity of mouse fibroblasts was assessed by MTT test by incubating the cells with PM-I, PMN-I, and PMN-II microgels at concentrations ranging from 5 to 50 μg/well for 7 days. As described in Figure 10, the proliferation of

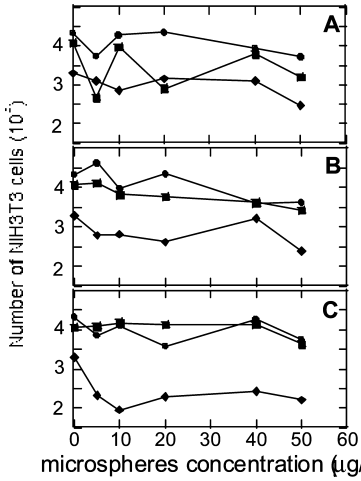

Figure 9. Viability of NIH3T3 mouse fibroblasts incubated with different amounts of PM-I (A), PMN-I (B), and PMN-II (C) for 4 h (●), 8 h (■), and 18 h (◆), respectively. Each well contained 0.5 mL of microspheres suspension.

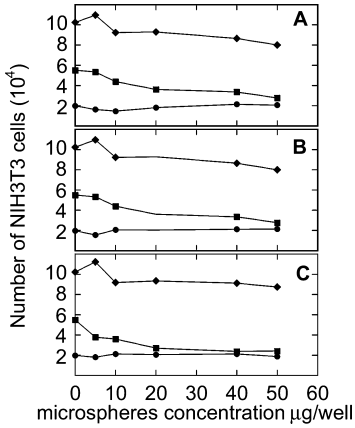

Figure 10. Proliferation of NIH3T3 mouse fibroblasts incubated with different amounts of PM-I (A), PMN-I (B), and PMN-II (C) for 4 h (●), 8 h (■), and 18 h (◆), respectively. Each well contained 0.5 mL of microspheres suspension.

NIH3T3 is not arrested regardless of the microgel type or quantity and it compares favorably with proliferation of same cells incubated in the absence of polymeric microgels.

In vitro biocompatibility tests allowed to assess that the interaction with these devices does not perturb the vitality and the proliferative activity of mouse fibroblasts and can be considered as potential injectable devices for further investigations on their impact on cell materials and tissues.

Concluding Remarks

The results described here are promising for the design of a new class of injectable drug delivery system based on the biocompatible PVA modified with the incorporation of the NiPAAm monomer in the microgel polymer network. Combining features such as dimensions in the micro/nanosize region and thermal responsivity in physiological conditions is the main characteristic of the microgels studied in this work. Water-in-water microemulsion technique provided an advantageous method to fabricate "soft" microdevices with low, if any, cytotoxicity. Morever, this approach to cross-link and incorporate NiPAAm allows an efficient control of the particles size by choosing the proper stirring speed. We showed that emulsification applying a higher shear speed yields smaller microgel spheres with a better defined size distribution and with an enhanced temperature response.

The hydrophilic anticancer case drug doxorubicin (DOXO) was loaded into the microgels. The release of DOXO at 25 °C (below LCST) was slower then at physiological temperature (above LCST), these results suggest that the DOXO drug release kinetics strongly depend on environmental temperature, the swelling, and the interactions of the loaded drug with microgels. Probable modulations in the behavior of differently modified thermoresponsive devices can be expected when surface charges or external molecules are included in the microgel network structure. However, in this work we were interested in the proof of concept concerning the possibility to use a handy and safe synthetic method as the "water-in-water" microemulsion polymerization to obtain thermoresponsive microgels spheres, tunable in size and in NiPAAm content.

This finding will lead us to design a microgel with implemented functionality by decorating the microgel surface with hyaluronic acid, a ligand of CD44 receptor, the membrane protein overexpressed in tumor cells. The modification of the microgels surface will increase the bioavailability of doxorubicin with a localized release of drug to the target cells. The same microgels represent a suitable platform for sensors functioning on fluorescence resonance energy transfer (FRET) effect,[39] on quantum dots technology,[16] and for magnetically responsive microactuators.[40]

Acknowledgment. This work has been partially funded by the international Ph.D. student program of the University of Rome Tor Vergata and MUIR-PRIN 2007LCNTW project. We thank Dr. E. Chiessi for helpful discussions, Dr. Prakash Wadgaonkar of Chemical National Laboratory, Pune, India, for elemental analysis measurements, and Dr. R. Pepi of TA Instruments for DSC analysis.

Supporting Information Available. Description of the dynamic light scattering results regarding the size distribution of PMN-I microgel spheres and its temperature dependence. This material is available free of charge via the Internet at http://pubs.acs.org.

References and Notes

(1) Dimitrov, I.; Trzebicka, B.; Muller, A. H. E.; Dworak, A.; Tsvetanov, C. B. *Prog. Polym. Sci.* **2007**, *32*, 1275–1343.
(2) Schmaljohann, D. *Adv. Drug Delivery Rev.* **2006**, *58*, 1655–1676.
(3) Qiu, Y.; Park, K. *Adv. Drug Delivery Rev.* **2001**, *53*, 321–339.
(4) Fundueanu, G.; Constantin, M.; Ascenzi, P. *Biomaterials* **2008**, *29*, 2767–2775.
(5) Henmei, N.; Kawagichi, H.; Endo, T. *Colloid Polym. Sci.* **2007**, *285*, 819–826.
(6) Constantin, M.; Fundueanu, G.; Bortolotti, F.; Cortesi, R.; Ascenzi, P.; Menegetti, E. *Int. J. Pharm.* **2007**, *330*, 129–137.
(7) Dufresne, M. H.; Le Garrec, D.; Sant, V.; Leroux, J. C.; Ranger, M. *Int. J. Pharm.* **2004**, *277*, 81–90.
(8) Fundueanu, G.; Constantin, M.; Bortolotti, F.; Ascenzi, P.; Cortesi, R.; Menegatti, E. *Macromol. Biosci.* **2005**, *5*, 955–964.
(9) Zhang, X. Z.; Chu, C. C. *Colloid Polym. Sci.* **2004**, *282*, 1415–1420.
(10) Zhang, X. Z.; Chu, C. C. *Am. J. Drug Delivery* **2005**, *3*, 55–65.
(11) Fang, S. J.; Kawaguchi, H. *Colloid Polym. Sci.* **2002**, *280*, 984–989.
(12) Zhang, J.; Xu, S.; Kumacheva, E. *J. Am. Chem. Soc.* **2004**, *126*, 7908–7914.
(13) Jackson, J. K.; Springate, M. K.; Hunter, W. L.; Burt, H. M. *Biomaterials* **2000**, *21*, 1483–1491.
(14) Vinogradov, S. V. *Curr. Pharm. Des.* **2006**, *12*, 4703–4712.
(15) Fujishige, S.; Kubota, K.; Ando, I. *J. Phys. Chem.* **1989**, *93*, 3311–3313.
(16) Jun, L.; Xia, H.; Yang, L. Y.; Di, L.; Yongwei, W.; Jinghong, L.; Yubai, B.; Tiejin, L. *Adv. Mater.* **2005**, *17*, 163–166.
(17) Fernandez-Nieves, A.; Fernandez-Barbero, A.; De las Nieves, F.; Vincent, B. *J. Phys.: Condens. Matter* **2000**, *12*, 3605.

(18) Fernandez-Barbero, A.; Fernandez-Nieves, A.; Grillo, I.; Lòpez Cabarcos, E. *Phys. Rev. E* **2002**, *66*, 051803−10.
(19) Rubio Retama, J.; Frick, B.; Seydel, T.; Stamm, M.; Fernandez Barbero, A.; Lòpez Cabarcos, E. *Macromolecules* **2008**, *41*, 4739–4745.
(20) Sierra-Martin, B.; Romero-Cano, M. S.; Cosgrove, T.; Vincent, B.; Frnandez-Barbero, A. *Macromolecules* **2005**, *38*, 10782–10787.
(21) Feil, H.; Bae, Y. H.; Feijen, J.; Kim, S. W. *Macromolecules* **1993**, *26*, 2496–2500.
(22) Cavalieri, F.; Chiessi, E.; Villa, R.; Vigano', L.; Zaffaroni, N.; Telling, M. F.; Paradossi, G. *Biomacromolecules,* **2008**, *9*, 1967–1973.
(23) Hacker, M. C.; Klouda, L.; Brandy, B. M.; Kretlow, J. D.; Mikos, A. G. *Biomacromolecules* **2008**, *9*, 1558–1570.
(24) Cavalieri, F.; Miano, F.; D'Antona, P.; Paradossi, G. *Biomacromolecules* **2004**, *5*, 2439–2446.
(25) van Dijk-Wolthuis, W. N. E.; Franssen, O.; Talsma, H.; van Stenbergen, M. J.; Kettenes-van den Bosh, J. J.; Hennink, W. E. *Macromolecules* **1995**, *28*, 6317–6322.
(26) van Dijk-Wolthuis, W. N. E.; Kettenes-van den Bosh, J. J.; van der Kerk-van Hoof, A.; Hennink, W. E. *Macromolecules* **1997**, *30*, 3411–3413.
(27) Franssen, O.; Hennink, W. E. *Int. J. Pharm.* **1998**, *168*, 1–7.
(28) De Belder, A. N.; Granath, K. *Carbohydr. Res.* **1973**, *30*, 375–378.
(29) Stenekes, R. J. H.; Hennink, W. E. *Int. J. Pharm.* **1999**, *189*, 131–135.
(30) Mossman, T. *J. Immunol. Methods* **1983**, *65*, 55–63.
(31) Robert, J. H.; Franssen, O.; Bommel, E. M. G.; Crommelin, D. J. A.; Hennink, W. E. *Pharm. Res.* **1998**, *14*, 557–561.
(32) Berne, B. J.; Pecora, R. *Dynamic Light Scattering*; Dover: Mineola, NY, 2000; p 196.
(33) Feil, H.; Bae, Y. H.; Feijen, J.; Kim, S. W. *Macromolecules* **1993**, *26*, 2496–2500.
(34) Brazel, C. S.; Peppas, N. A. *Macromolecules* **1995**, *28*, 8016–8020.
(35) Schott, H. *J. Macromol. Sci., Part B: Phys.* **1992**, *31* (1), 1–9.
(36) Liu, S. Q.; Yang, Y. Y.; Liu, X. M.; Tong, Y. W. *Biomacromolecules* **2003**, *4*, 1784–1793.
(37) Brazel, C. S.; Peppas, N. A. *J. Controlled Release* **1996**, *39*, 57–64.
(38) Gutowska, A.; Bae, Y. H.; Feisen, J.; Kim, S. W. *J. Controlled Release* **1992**, *22*, 95–104.
(39) Jones, C. D.; McGrath, J. G.; Lyon, L. A. *J. Phys. Chem. B* **2004**, *108*, 12652–12657.
(40) Liu, T. U.; Hu, S. H.; Liu, K. H.; Shaiu, R. S.; Liu, D. M.; Chen, S. Y. *Langmuir* **2008**, *24*, 13306–13311.

BM900185U